Engineering and Technology Journal
Journal homepage: https://etj.uotechnology.edu.iq

Adaptive Neuro-Fuzzy Voltage Control for LCL-Filter Grid-Connected Converter

Safa S. Olwie*, Abdulrahim T. Humod, Fadhil A. Hasan

Electrical Engineering Dept., University of Technology-Iraq, Alsina'a street, 10066 Baghdad, Iraq.
*Corresponding author Email: eee.19.12@grad.uotechnology.edu.iq

HIGHLIGHTS

- This paper presents how voltage is affected by increased loads or voltage sag.
- The Adaptive neuro-Fuzzy Inference System (ANFIS) is used as an Intelligent controller.
- The mathematical models for the LCL filter are investigated.
- The proposed approach shows more effective results than previous performance for voltage controlling and harmonic reduction.

ARTICLE INFO

Handling editor: Jawad K. Ali

Keywords:
Distributed power generation; LCL filter; mathematical models of LCL filter; PI control; ANFIS.

ABSTRACT

Inductance – Capacitance – Inductance (LCL) filter is a very attractive candidate for renewable energy system applications due to its high efficiency. High attenuation of the switching frequency harmonics, small size, low fee, and improving the overall harmonic distortion (THD). This paper presents how voltage is affected by increased loads or voltage sag. Therefore it is necessary to control it with certain controllers. The Adaptive Neuro-Fuzzy Inference System (ANFIS) is used as an intelligent controller, the voltage constraint as training data for ANFIS obtained from PI. The filter works in a good connection between the inverter and the grid and rewords unwanted harmonics from using the inverter. The mathematical models for the LCL filter are investigated. The proposed approach shows more effective results than previous performance for voltage controlling and harmonic reduction. It gives overshoot (0.5%), steady state error (0.005), settling time (0.03 sec), rise time (0.005 sec), and improving THD 8.67% to 2.33% by comparing these results of ANFIS respectively with the results of PI which gave(3%),(0.01),(0.2sec)and(0.02sec).

1. Introduction

Nowadays, power plants used distributed Generations (DGs) systems because of thier reliability and low gas emission, which reduce pollution and make theme environmentally friendly, in addition to the most important factor, which is the low cost compared to conventional electricity source. Connected to DGs devices low voltage distribution device for renewable energy supply which include; fuel cellular, wind energies or PV, to the grid using power converter [1]. As we know

That renewable energy sources generate DC voltage, it is necessary to use a power converter to convert it into AC voltage, so that it can be injected into the network when needed, Rreasons for using the inverter commonly in renewable energy systems [2]. In DG applications, VSI is very good at controlling the power injected into the network; still the pulse width modulation method of the VSI leads to the emergence of unwanted high and low harmonics [3, 4]. Characteristics and specifications of each type of filter were shown through previous research.

Although a single inductor L-filter out is popular and easy to use, it has low attenuation and excessive inductance price. The voltage drop across the inductor makes poor gadget dynamics, causing an extended-time response. Using L-filter out, the inverter switching frequency must have an excessive value sufficiently to attenuate the harmonics [5] sufficiently.

L-type filters can attenuate -20 dB/dc, which is a small amount, so it needs a capacitor that produces a large and high impedance within the frequency range. The LC filter is ideal for modulations with relatively high load impedance and above operating frequency. After that, it needs a large capacitance to reduce losses and thus cost. Ventilated too large is not encouraged to avoid

http://doi.org/10.30684/etj.2022.132342.1115
Received 04 December 2021; Accepted 08 June 2022; Available online 01 October 2022
2412-0758/University of Technology-Iraq, Baghdad, Iraq

Nevertheless, it should not be excessive in the amplifier because it will lead to the appearance of the inrush current, Also it will increase in the reactive power, especially at the original frequency, in addition to the possibility of the appearance and phenomenon of resonance on the side of the network, Furthermore, if. The LC filter is placed between any system and the network, the resonant frequency changes over time because the inductance will also change in its price [6].

LCL-filter can use and provide a solution for the high capacitance, because it has a better decoupling between the converter and the grid impedance, better attenuation of the switching frequency harmonics, and improves the Total Harmonic Distortion (THD). This leads to a decrease in size and costs. However, due to filter's resonance, the system's stability will be affected; passive damping is used connecting resistors in parallel with the filter capacitors to dampen the resonance harmonics [7].

This work proposed the best way to control voltage variation, making its value constant even for changing loads, getting rid of the harmonic and reducing the THD to less than 5% through an LCL filter between the inverter and the grid. Although the voltage control is proposed using PI controller, it has taken adelayed time to reach a steady state in addition to the sensitivity of Ki and Kp factors (parameters of PI controller) and moreover, due to the sudden voltage change, it gets little response. Among the special smart controllers, ANFIS it characterized by fast performance, insensitivity to Ki and Kp factors, stability even when changing the load, and simplicity in installation. Decoupling control is used. The important distinguishing characteristic should be iq = 0, which gives the idea an easy configuration and secure manipulation.

This search was completed as follows: in part 2 the mathematical impersonation of the LCL-filter between converter and network.Then the equations for the system are obtained using the direct decoupling method. Next, section 3 represents an overview of the PI and ANFIS. Finally, section 4 represents the simulation results for each controller PI and ANFIS and compares them.

2. Mathematical Model of Lcl Filter Inverter

The stationary body analysis of the network may be expressed in Figure 1. The usage of Kirchhoff's voltage regulation is as follows:

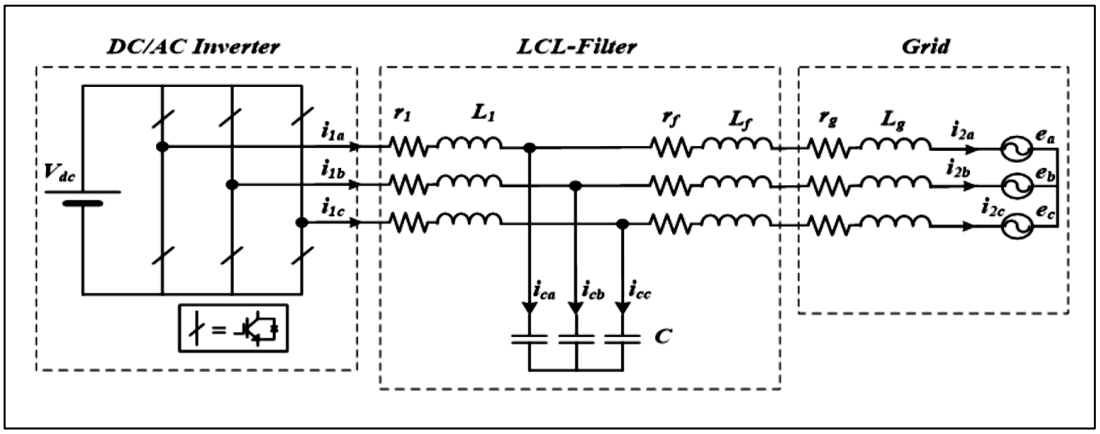

Figure 1: LCL-filter grid-connected converter

$$\tilde{v}_1 - r_1\tilde{i}_1 - L_1\rho\tilde{i}_1 - \tilde{v}_c = 0 \quad (1)$$

$$\tilde{v}_1 - \tilde{v}_c = L_1\rho\tilde{i}_1 + r_1\tilde{i}_1 \quad (2)$$

$$\tilde{v}_c - r_2\tilde{i}_2 - L_2\rho\tilde{i}_2 - \tilde{e} = 0 \quad (3)$$

$$\tilde{v}_c - \tilde{e} = L_2\rho\tilde{i}_2 + r_2\tilde{i}_2 \quad (4)$$

Where: $\tilde{i}_1 = \tilde{i}_c + \tilde{i}_2$, $\tilde{i}_c = C\rho\tilde{v}_c$, $L_2 = L_f + L_g$, $r_2 = r_f + r_g$, ρ: the derivative factor, $\tilde{v}_1$: the voltage of the converter side, $\tilde{i}_1$: the current of converter side, $\tilde{v}_c$: the voltage of capacitance, $\tilde{i}_c$: the current of capacitance, $\tilde{i}_2$: the current of the grid, L_1 : the inductance of converter side filter, L_f : the inductance of grid side filter, L_g : the inductance of grid, r_1 : the resistance of converter side filter, r_f : the resistance of grid side filter, r_g : the resistance of the grid.

Phase-lock loop (PLL) is synchronized with the voltage of the grid and phase angle found totally at the direct-quadrature (d-q) frame using Park's Transformation. The d-q domain was used because it is simple and excellent in dynamic response [8]. To convert quantities from d-q to abc, a phase angle is needed for the conversion obtained from PLL. A usually adopted technique in analysing 3-phase structures is to use an αβ and dq frame Figure 2.

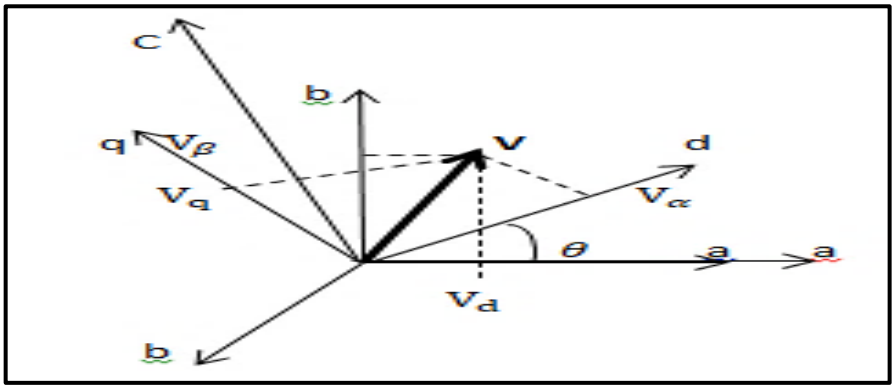

Figure 2: αβ and dq frame

The mathematical model inside the αβ frame is:

$$V_{1\alpha\beta} - V_{c\alpha\beta} = r_1 i_{1\alpha\beta} + L_1 \rho i_{1\alpha\beta} \quad (5)$$

$$V_{c\alpha\beta} - e_{\alpha\beta} = r_2 i_{2\alpha\beta} + L_2 \rho i_{2\alpha\beta} \quad (6)$$

$$i_{c\alpha\beta} = C\rho V_{c\alpha\beta} \quad (7)$$

$$i_{1\alpha\beta} = i_{c\alpha\beta} + i_{2\alpha\beta} \quad (8)$$

It is important to note that the two-phase d-q system has a property, which is that any vector has an amount that rotates with the frame and with the same velocity, which is the angular velocity ω, and the equations are as follows:

$$V_{1d} - V_{cd} = r_1 i_{1d} + L_1 \rho i_{1d} - L_1 \omega i_{1d} \quad (9)$$

$$V_{1q} - V_{cq} = r_1 i_{1q} + L_1 \rho i_{1q} + L_1 \omega i_{1q} \quad (10)$$

$$V_{cd} - e_d = r_2 i_{2d} + L_2 \rho i_{2d} - L_2 \omega i_{2d} \quad (11)$$

$$V_{cq} - e_q = r_2 i_{2q} + L_2 \rho i_{2q} + L_2 \omega i_{2q} \quad (12)$$

Where: $i_{cd} = C\rho V_d$, $i_{cq} = C\rho V_q$, The decoupling components are defined: $i_{1d}{}^{decoupled} = \omega L_1 i_{q1}$, $i_{q1}{}^{decoupled} = -\omega L_1 i_{d1}$, so the currents will be :

$$i_{1d} = i_{cd} + i_{2d} + \omega L_1 i_{q1} \quad (13)$$

$$i_{1q} = i_{cq} + i_{2q} - \omega L_1 i_{1d} \quad (14)$$

3. Pi and Adaptive Neuro-Fuzzy Inference System (ANFIS)

PI controllers are the most popular and widely used in most power electronic closed loop appliances. It has capabilities in controlling linear plants, from slow to fast systems. The benefits of adaptive PI controllers are avoiding time-ingesting and difficult guide adjustment of accuracy through presenting the optimum putting PI controllers settings robotically as machine dynamics or exchange working points[9]. However, constant PI coefficients should be based on an accurate mathematical model to ensure control performance. This is difficult due to the change of loads and, consequently, the change of voltage. In other words, it is the fixed transactions of a conventional file that the directional field control-based PI controller cannot be unsure of System power [10]. The shape schematic of the voltage manipulates gadget for LCL filter-based totally grid-related inverter display in Figure3.

With the fast growth of artificial intelligence in controllers, fuzzy logic and ANFIS are available in more precise inverter voltage and current controls. It can deal with non-linear systems more accurately and quickly, thus maintaining voltage stability and stabilizing the system. ANFIS can be used in automated applications and suggests control and signal processing. ANFIS, known by Hang in 1993, combines the advantages of NN and FLC and thus its implementation in one control. ANFIS is a fuzzy system that simplifies the complexities of the control system through data processing and is based on the concept of Artificial Neural networks (ANN). In ANFIS, a fuzzy inference mechanism by structure and an advanced adaptive NN feeding neuron are embedded [11-23]. The ANFIS system was used to increase the quality of control and thus increase efficiency without the need to know the internal details such as its control unit's parameters and feedback parameters. [24]. A machine or a controller may be developed by combining the functions of fuzzy good judgment and neural community strategies, which has an overall performance compared to the simplest fuzzy good judgment gadget. This is referred to as ANFIS [25]. ANFIS is the

plainness of its enforcement, better than others in the speed of performance, durability, and strength, and it does not depend on parameters and load changes.

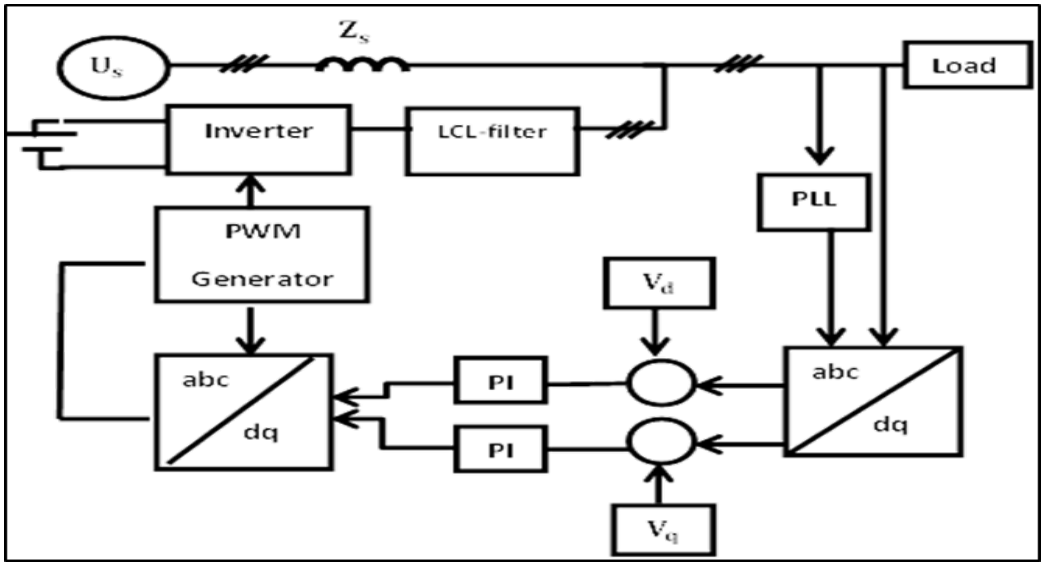

Figure 3: Structure schematic of the control system

4. Results and Discussion

4.1 Determination of The Parameters of The LCL- Filter

The designed parameters of the LCL filter are listed regardless of the used control methods. The parameters are calculated based on the inverter specification listed in Table 1. The LCL filter, which filters out unwanted high and very low frequencies, requires parameters to be found. The inductance values on both sides and the amplitude and the rest of the parameters must be known. The following equations are used to find them.

Table 1: Inverter specification

Parameters	Physical meaning	Value
f_s	Switching frequency	10 kHz
f_n	Utility frequency	50 Hz
V_{dc}	DC-link	600 V
V_{gll}	Utility line voltage	380 V
P_n	Inverter-rated output power	100 kW

For a current ripple peak of 10% of the rated current, the inverter side inductance L1 is calculated depending on Equation (15) [26].

$$L_1 = \frac{V_g}{2\sqrt{6}\, f_s\ i_{rippl,peak}} \tag{15}$$

Where: Vg is the grid rms phase voltage and f_s is the inverter switching frequency. Filter capacitance is calculated by considering the maximum power factor variation, commonly set at 5% for GCI [27].

$$C \leq 0.05 C_b \tag{16}$$

Where $C_b = \frac{1}{\omega_n Z_b}$ is the base capacitance and $Zb = \frac{V_{gll}{}^2}{Pn}$ is the base impedance, V_{gll} is a grid line voltage, P_n is inverter-rated power, and $\omega_n = 2\pi f_n$ is the natural frequency [27].

Similarly, for an LCL filter, the total inductance limit L_2 must be determined. The IEEE-519 harmonic restrictions are used.

$$L_2 = 0.2888 L_1 \tag{17}$$

Where (0.2888) is a ratio index that measures inductance on the inverter and the grid sides.The parameter values of the LCL filter can be arranged in Table 2:

Table 2: The LCL filter parameters

Parameters	Physical meaning	Value
Zb	Base impedance	1.444 Ω
ω_n	Natural frequency	314.159 rad/sec
C_b	Base capacitance	2.204 mF
C	Filter capacitance	0.1102 mF
I_{ratad}	Rated current	263.157 A
I	Phase current	151.934 A
i_{ripple}	Ripple current	22.7901 A
L_1	Inductance of the inverter side	0.5305mH
L_2	Inductance of the grid side	0.0567mH

4.2 Simulation of Voltage Control with The PI Controller

The voltage applied to the inductive and motor loads comes from the grid generator. As a result of load variation, a voltage change on the load will accrue. To reduce this variation, the injected power from the inverter will be controlled using a PI controller. Figure 4 depicts the model in the Matlab 2017a /Simulink, which was implemented considering the values in Tables 1 and 2. The Simulink model in Figure 4 consists of two reference voltage inputs which are a direct voltage ($V_d = 1$) and a quadratic voltage ($V_q = 0$), Two controllers (PI controllers) for V_d and V_q. The PLL, voltage and current transformations, and LCL filters connected in series between the inverter and the grid, which has a three-phase generator producing 380 V, are used to feed two loads. The first is a three-phase series inductive load and the second is an asynchronous motor that runs in a specific time (0.2sec to 0.4 sec). The simulation results were obtained from the Matlab/Simulink software package under abnormal grid operating conditions with constant grid voltage magnitude, frequency, and power from the DC source.

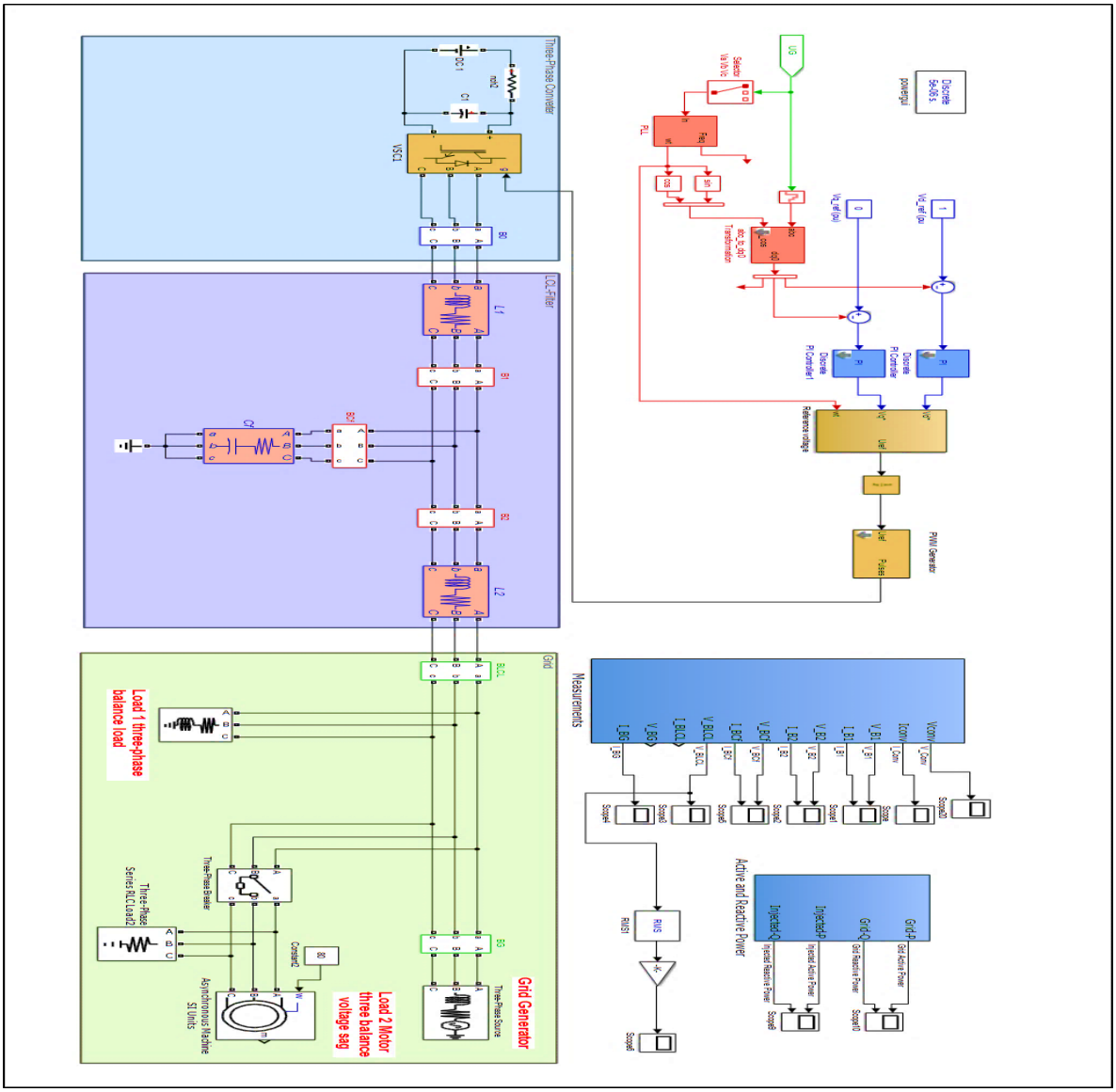

Figure 4: Simulation model of the LCL-filter Grid-Connected Converter with the PI controller

Figure 5.a shows the converter voltage before the LCL filter for the time from (0 to 0.1 sec). Figure 5.b illustrates the current from (0 to 0.6 sec), where during this time, the load is varied from o.2 sec to 0.4 sec due to the operation of the motor. The inverter specifications are as follows: The DC-link voltage is 600 volts, and the switching frequency is 10 kHz. The utility frequency is 50 kHz. The inverter's output power is rated at 100 kW.

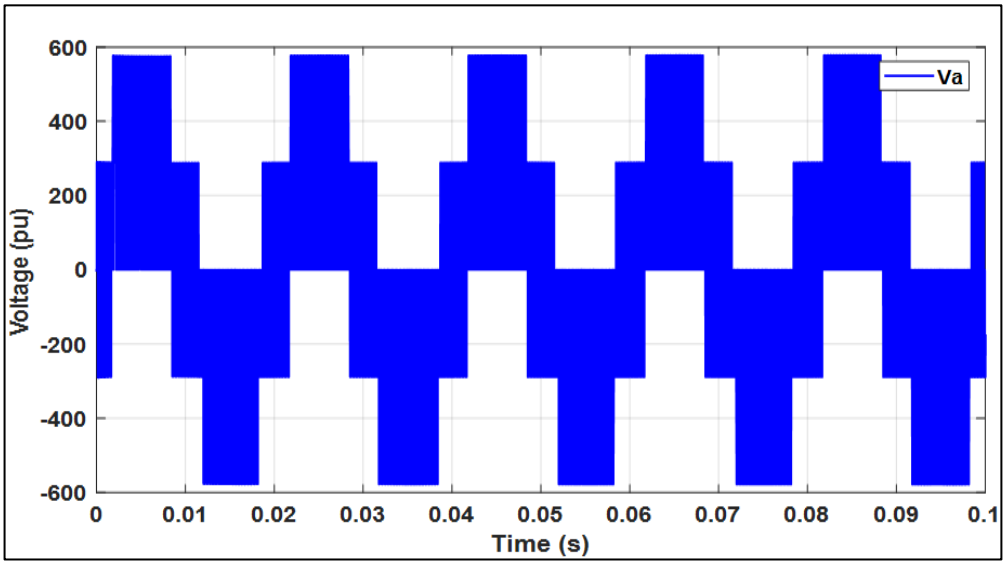

(a)

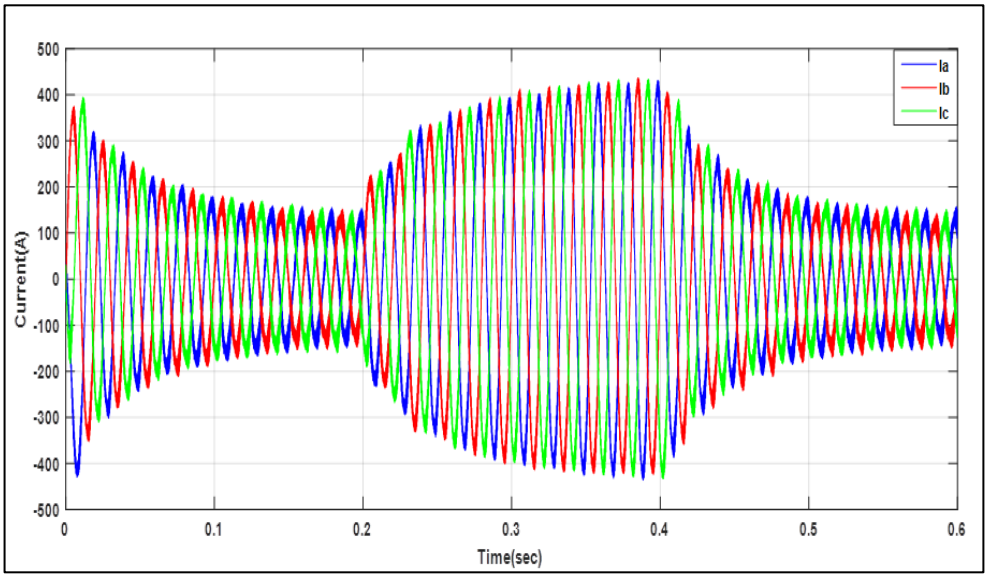

(b)

Figure 5: Converter: (a) voltage phase a (pu) (b)) three-phase current

The grid voltage and the current waveform are shown in Figure 6. The waveforms are sinusoidal and contain few harmonics. Figure 6.a shows the three-phase voltage waveform during the balanced voltage sag disturbance from (0.2 to 0.4) sec. It can be seen that the voltage magnitude in all the phases is reduced equally, but the waveforms are not distorted while the voltage amplitude is 380. Figure 6.b shows the three-phase current waveform during the voltage sag. There is an increase in the current magnitude during the fault at a time interval of 0.2-0.4 seconds. This is because the same amount of active power flows from the DC source to the grid before and during the voltage sag. Therefore, when the voltage decreases, the current has to increase to maintain active power flow. The peak current amplitude at a steady state is 135 A. Table 3 shows the values of the PI controller parameters obtained by the trial and error method.

Table 3: PI controller parameters for the voltage control method

Parameters	***kp***	***ki***
d-axi voltage controller	0.3	100
q-axis voltage controller	0.3	100

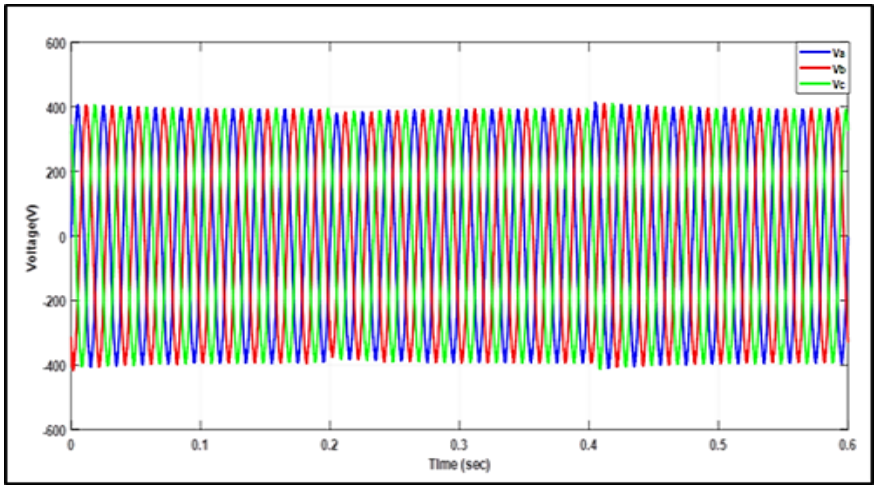

(a)

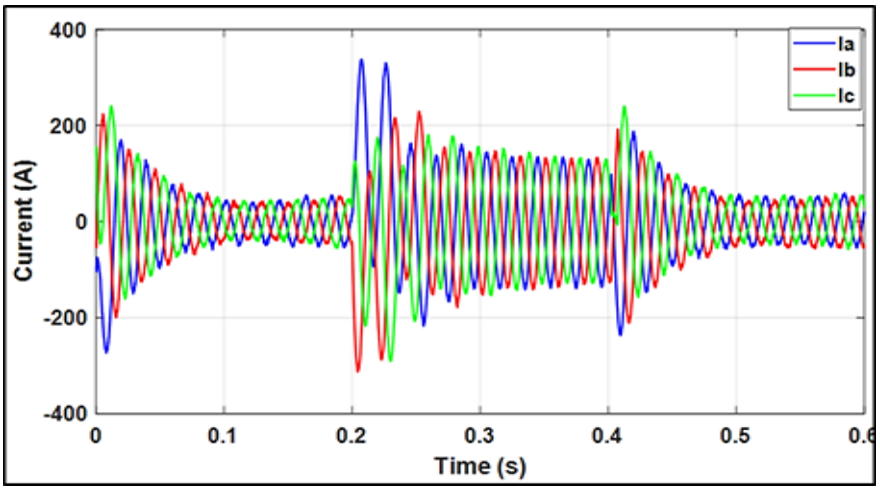

(b)

Figure 6: Grid (a) three-phase voltage (b) three-phase current

Figure 7 shows the response of the voltage RMS value for the LCL filter. The performance of the LCL filter after using the PI controller for the inverter. The RMS response has the following specifications:

Undershoot = 2.5%, Settling time = 0.15 sec, Steady state error = 0.01, and Peak time =0.018 sec. The following specifications are calculated for interring the motor load to the system and removing the motor load from the system. Overshoot = 3%, Settling time = 0.15 sec, Steady state error = 0.01, and Peak time =0.02 sec. In the controller, the voltage values are expressed per unit, the reference voltage equal to 1 p.u. The PI controller is a manually tuned method using trial and error to obtain zero error between the reference and the actual voltage. The results show that this was achieved.

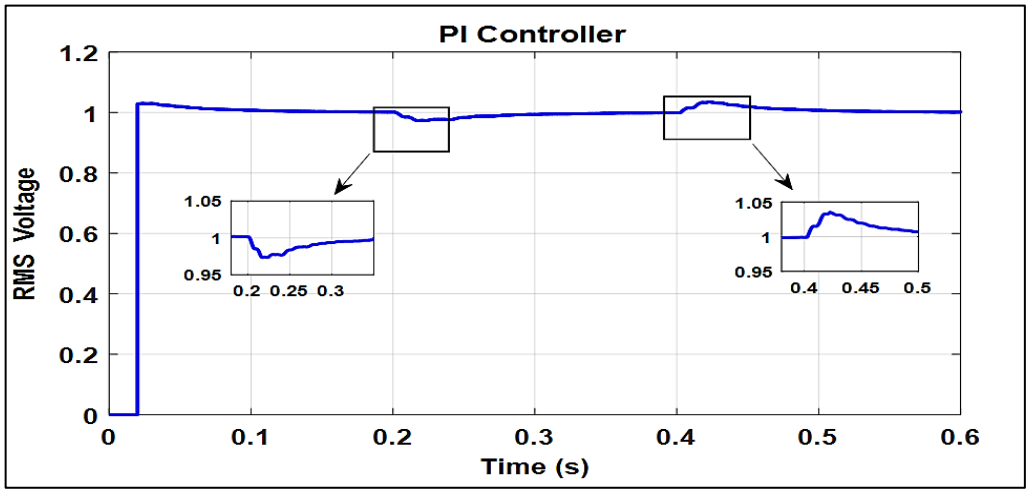

Figure 7: RMS voltage of LCL filter

Figure 8 shows the effect of the LCL filter using the PI controller for the inverter to reduce high harmonics and to keep the required fundamental harmonic by analyzing the harmonic of the converter current and the filter current. As a result, THD was reduced from 13.00% to 3.21%, which is allowed by IEEE 519-1992 standards since THD is less than 5%.

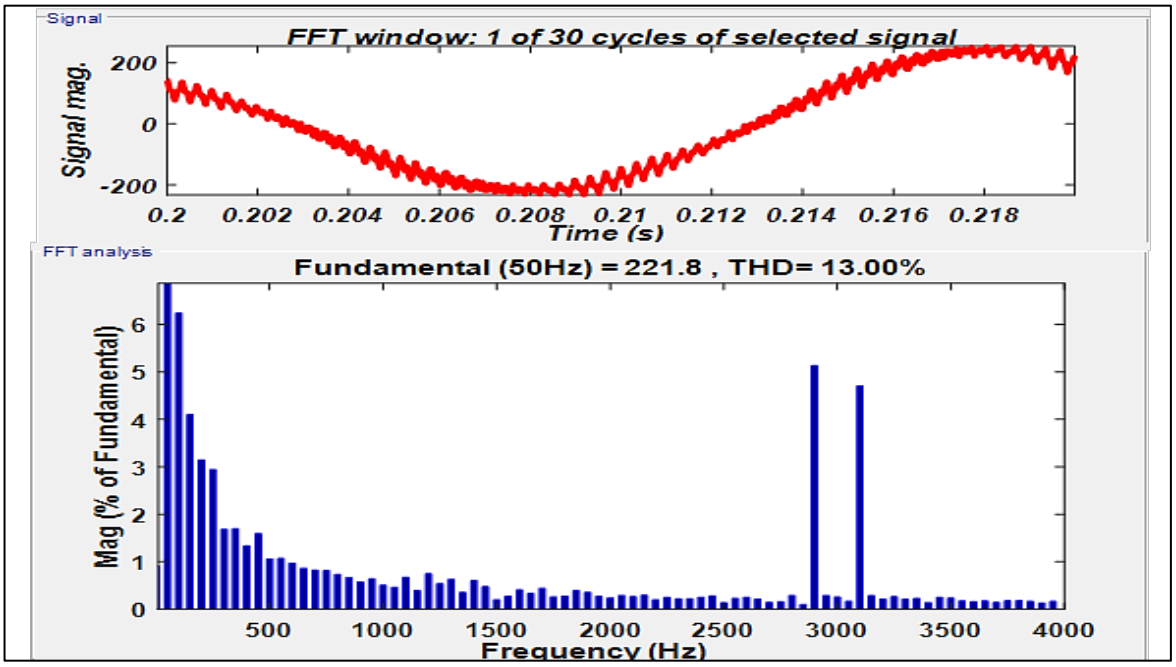

(a)

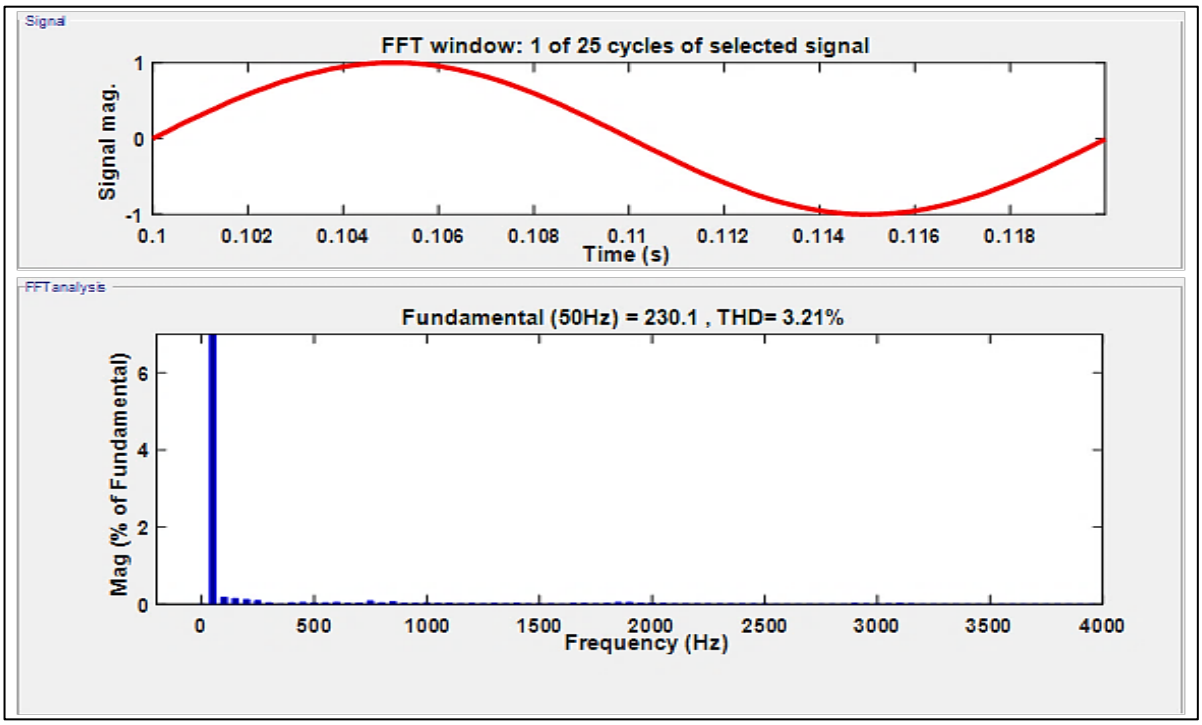

(b)

Figure 8: FFT (a) Converter current (b) LCL filter current

Despite the advantage stated previously, the PI controller has drawbacks, such as a long settling time and a large overshoot and undershoots, so it is required to choose another controller.

Figure 9 shows the grid power and the injected active power. The demand power is not injected in the manner as required.

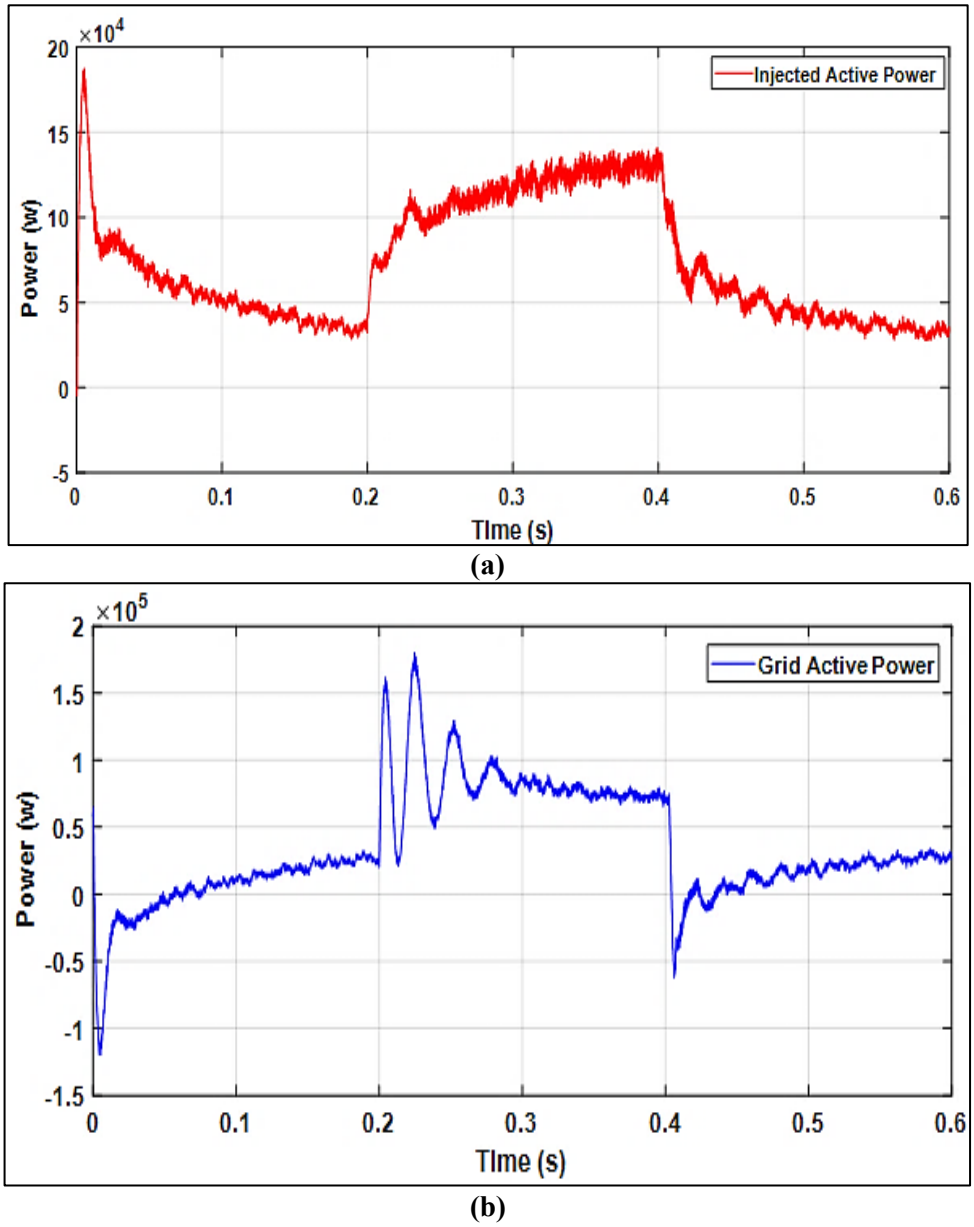

Figure 9: (a) Grid active power (b) Injected active power

4.3 Simulation of Voltage Control with The ANFIS Controller

Two controllers are utilized, including ANFIS, as shown in Figure 10. The ANFIS was performed with a block that has two inputs: error and integral of the error. The network is trained using a subtractive clustering algorithm. The steps for ANFIS controller training must apply.

The input and output data for the PI controllers in the previous Section II were transformed into a workspace to be used as desired data for ANFIS controllers. Using the command (anfisedit) in the command window and then clicking Enter, a new window, as illustrated in Figure11, will open. The following parameters are used to run the training process: Squash factor = 1.25, Accept ratio = 0.1, Reject ratio = 0.05 and Range of Influence = 0.2, after loading the data and pressing sub-clustering. After entering the error tolerance=0 and epochs= 10, press the button (Generate FIS) to start the training. When the training is completed, exit the window, save, and then set the result in the fuzzy logic block.

By pressing the button in Figure 11, the ANFIS structure appears as in Figure 12, containing the input and the base functions. The input and output are represented by the black balls. The white balls represent the input and output memberships, respectively. The blue balls represent the ANFIS controller's rules.

After running the program and testing the dynamic controller performance under unbalanced conditions, the converter voltage before the LCL filter is shown in Figure13.a during the period from (0 to 0.1 sec). Figure13.b shows the current from 0 to 0.6 seconds, during which the load varies from 0.2 to 0.4 seconds due to the motor's functioning. The inverter's parameters are as follows: The switching frequency is 10 kHz, and the DC-link voltage is 600 volts. 50 kHz is the utility frequency. The output power of the inverter is rated at 100 kW.

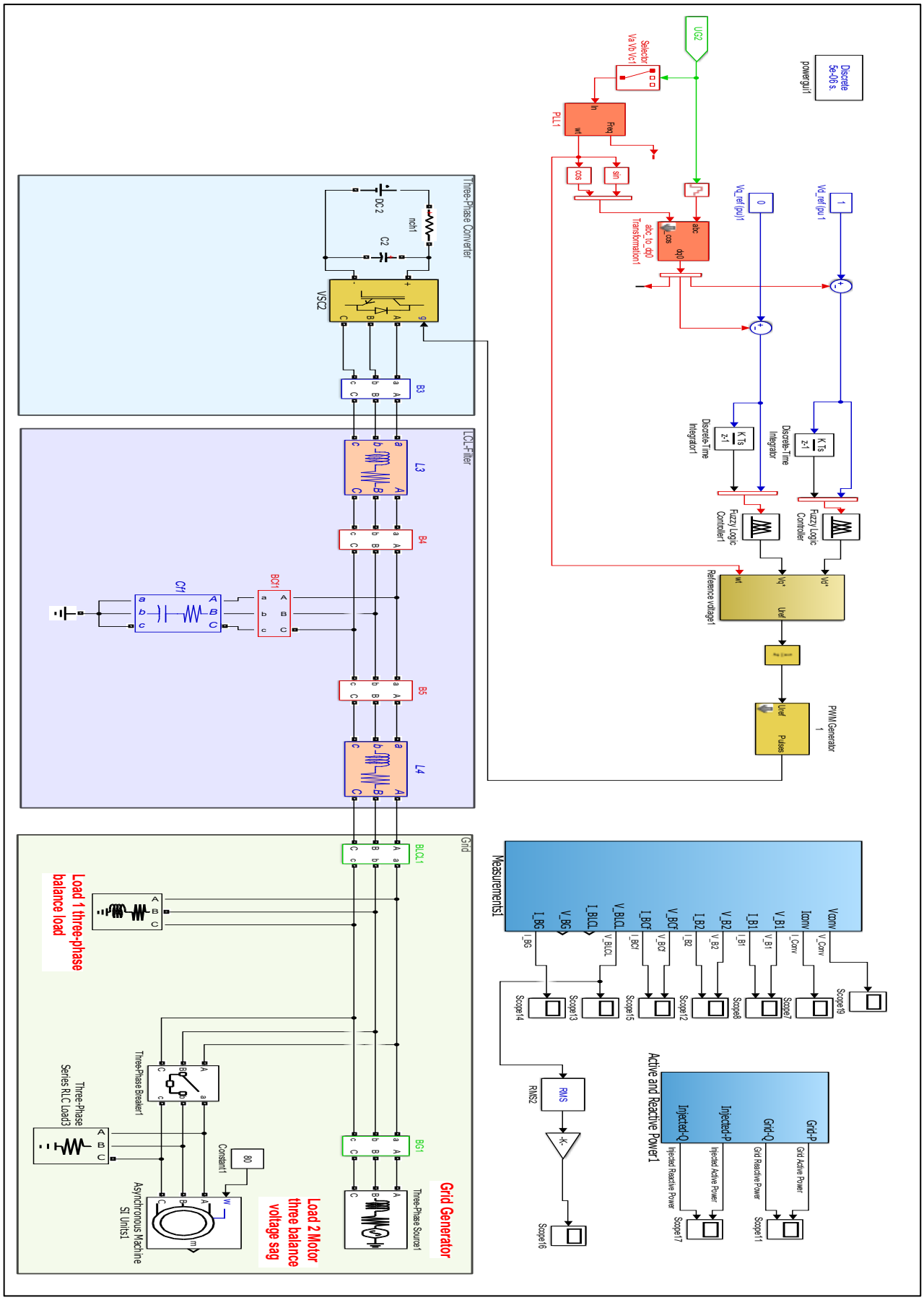

Figure 10: Simulink of the ANFIS controller with the LCL grid-connected inverter

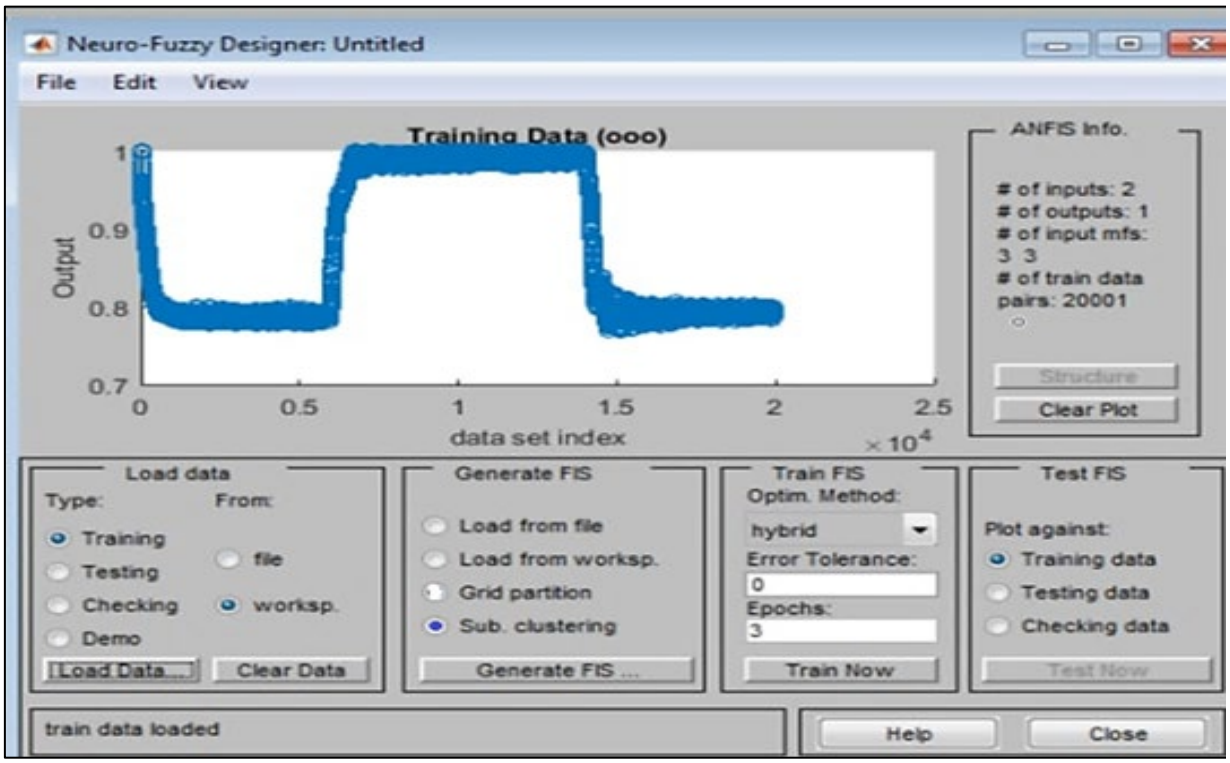

(a)

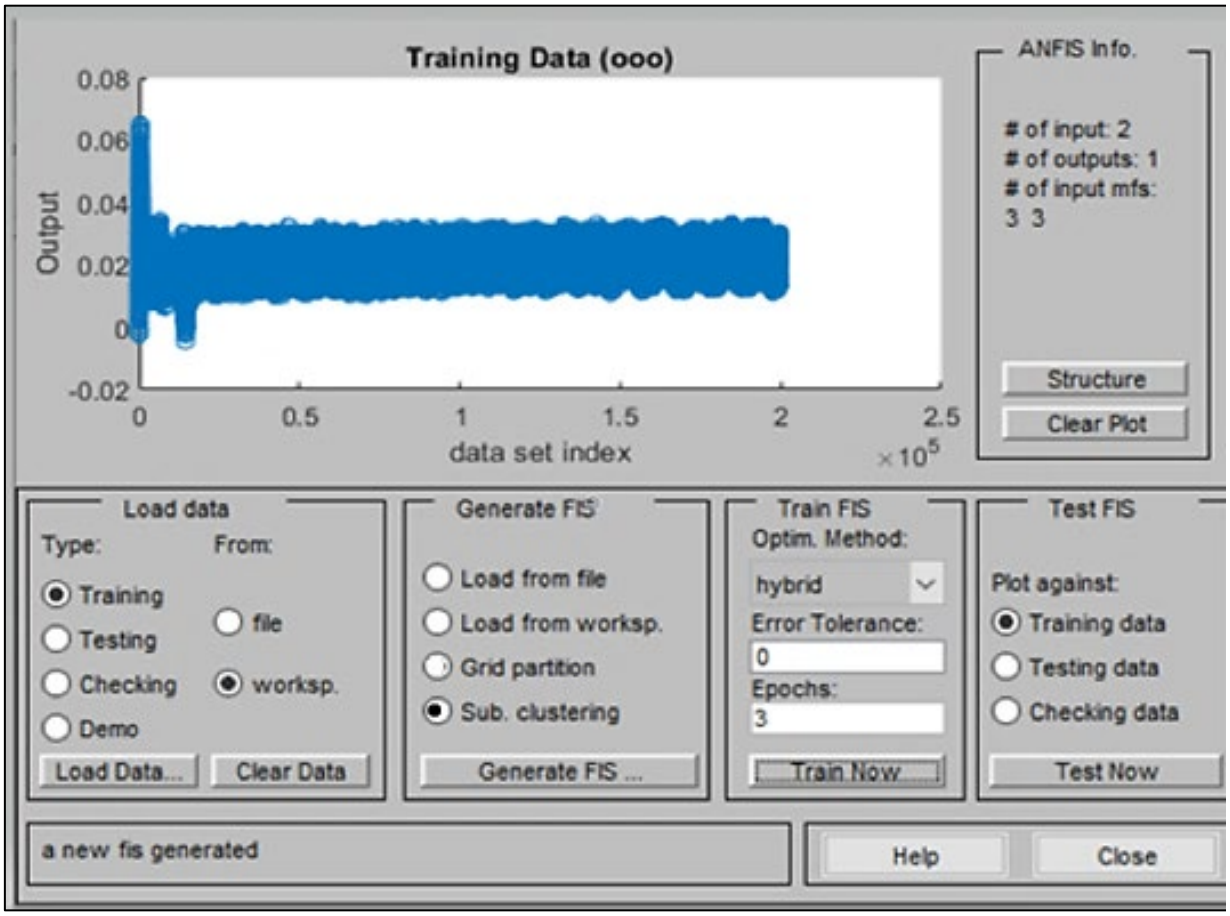

(b)

Figure 11: Loading data for the PI controller (a): D-axis and (b): Q-axis

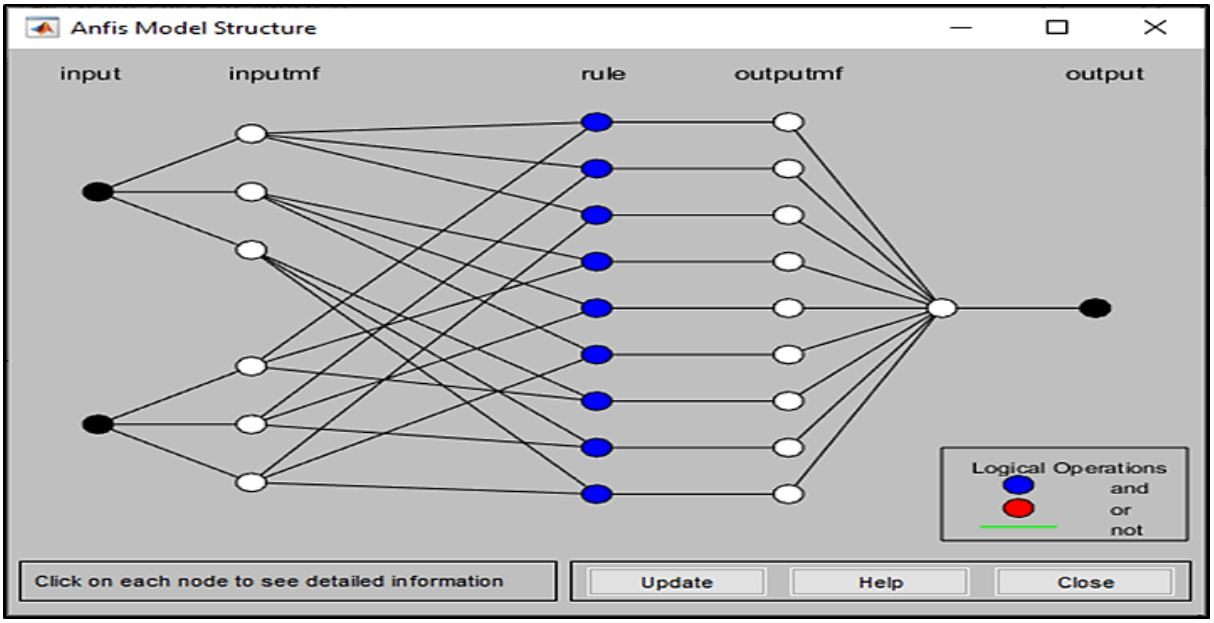

Figure 12: .Structure of ANFIS

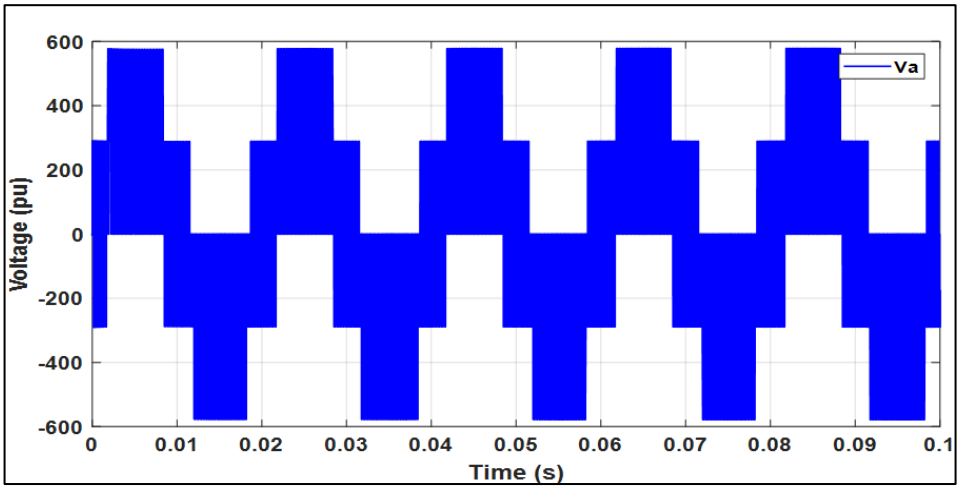

(a)

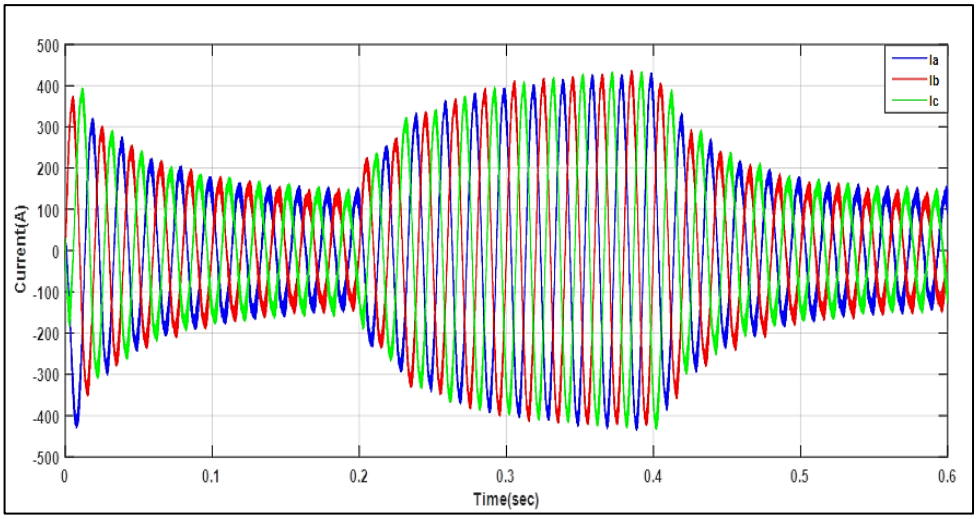

(b)

Figure 13: Converter: (a) Voltage phase a (pu) (b) Three phase current

Figure 14 shows the response of the voltage RMS value for the LCL filter. The performance of the LCL filter after using the ANFIS controller for the inverter. The RMS response has the following specifications:

Undershoot = 0.002%, Settling time = 0.05 sec, Steady state error = 0.001, and Peak time =0.008 sec. The following specifications are calculated for interring the motor load to the system and removing the motor load from the system. Overshoot = 0.005%, Settling time = 0.02 sec, Steady state error = 0.001, Peak time =0.02 sec.

Figure 15 shows the effect of the LCL filter using the PI controller for the inverter to reduce high harmonics and to keep the required fundamental harmonic by analyzing the harmonic of the converter current and the filter current. After using the ANFIS Controller, THD was reduced from 13.00% to 2.33%.

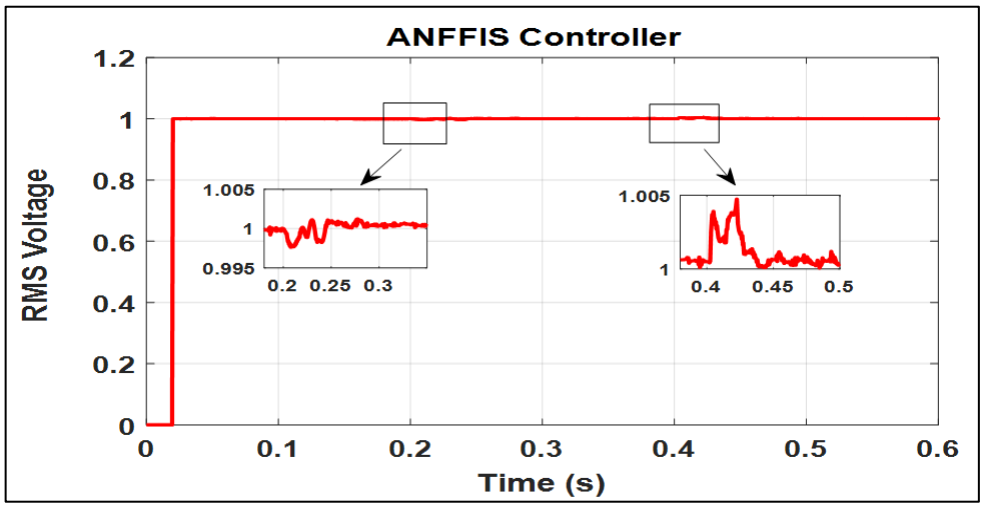

Figure 14: . RMS voltage for LCL filter (pu)

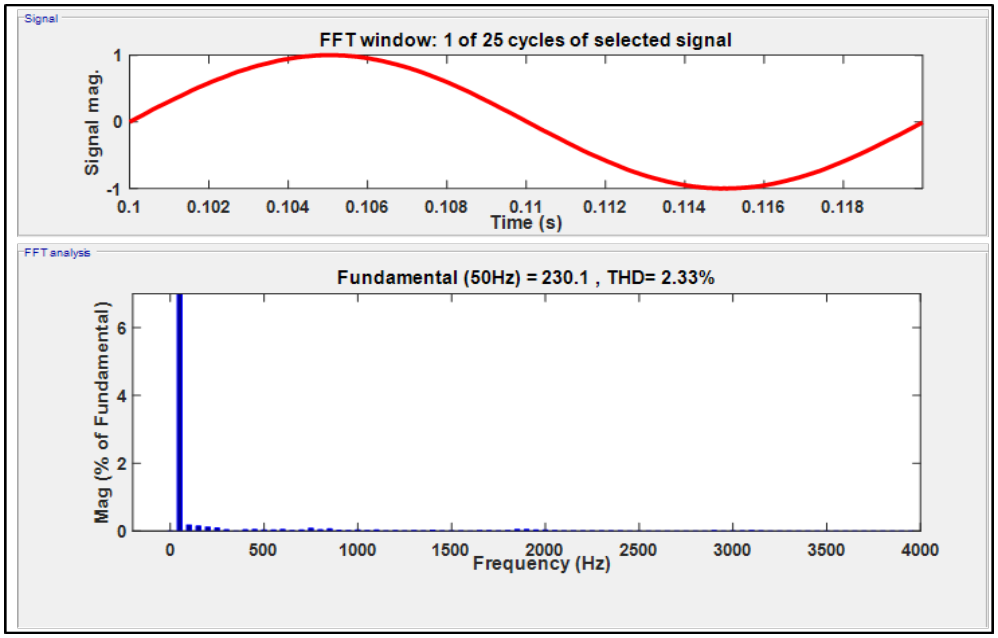

Figure 15: FFT for the LCL filter current

Figures 16.a and 16.b show the three-phase grid voltage waveform and the three-phase current waveform using the ANFIS controller. To test the effectiveness of the adaptive control with abnormal conditions, Figure 16.a shows the three-phase voltage waveform during the balanced voltage sag disturbance from (0.2 to 0.4) sec. It can be seen that the voltage magnitude in all the phases remained stable and was not affected by high loads even after entering the network and leaving work, while the voltage amplitude was 380. Figure 6.b shows the three-phase current waveform during the voltage sag. There is an increase in the current magnitude during the fault at a time interval of 0.2-0.4 seconds. This is because the same amount of active power flows from the DC source to the grid before and during the voltage sag.

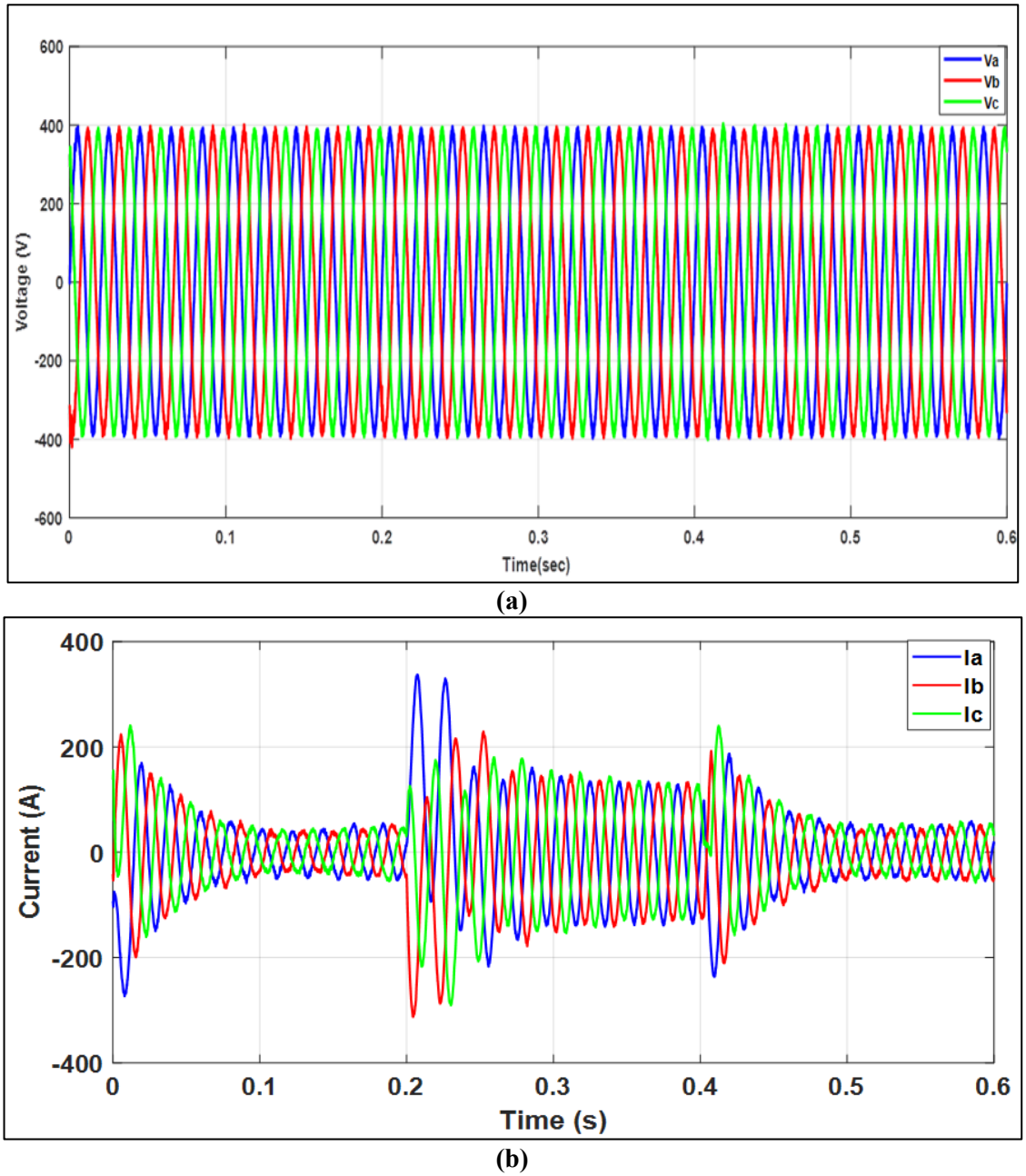

Figure 16: Grid (a) Three-phase voltage (b) Three-phase current

4.4 Comparison Between PI and ANFIS

The ANFIS controller started to replace the PI controller in a different application, including grid-connected voltage control. The voltage control method was good when using the PI controller to reduce the voltage sag that occurred when an error appeared or loads increased on the network. Still, it gave much better results when using ANFIS, as the voltage was kept almost constant, and the reduction in harmonics was less than 5%. A reduction in THD from 3.21% to 2.33% was observed. Figure17 shows the RMS voltage response for both the PI and the ANFIS controllers. The figure shows that the response of the ANFIS controller is better than the response of the PI controller, especially at the load variation. Table 4 compares RMS voltage responses for PI and ANFIS controllers in addition to load and exit. From the results of Table 4, it was observed that ANFIS is much better than the PI. From the results of Table 4, when Addition of load at 0.2 sec, it was noticed that the undershoot when using ANFIS is much less than the PI by 0.9992%, and the settling time (s) for PI at a steady state error of 0.01 is 0.15 sec, and for ANFIS control at steady state error of 0.001 is 0.05 sec. Peak time (s): 0.018 sec to 0.008 sec.

When the load exits in 0.4 sec, the overshoot when using ANFIS is 0.9998% less than when using PI, and the settling time (s) for PI at a steady state error of 0.01 is 0.15 sec, and for ANFIS control at a steady state error of 0.001 is 0.02 sec. Peak time (s) is the same 0.02 sec for two controllers.

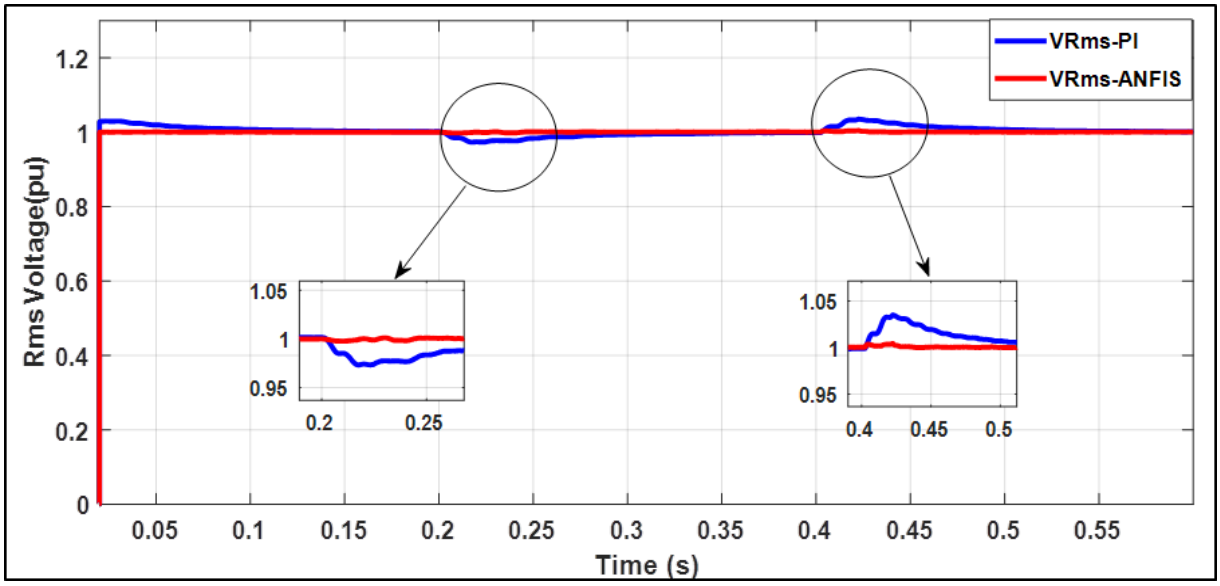

Figure 17: LCL filter RMS voltage for PI and ANFIS

Table 4: RMS voltage responses for PI and ANFIS controllers

Specifications	**At Addition to load**		**At the exit of the load**	
	PI controller	***ANFIS controller***	***PI controller***	***ANFIS controller***
Undershoot or overshoot	2.5%	0.002%	3%	0.005%
Settling time(s)	0.15 at Steady state error 0.01	0.05 at Steady state error 0.001	0.15 at Steady state error 0.01	0.02 at Steady state error 0.001
Peak time (s)	0.018	0.008	o.o2%	0.02

5. Conclusion

To find out the best type of filter suitable for the network, the types of filters, their work, and their applications were reviewed. The type of filter LCL was chosen for use in renewable energies applications because of its high features. The mathematical representation of the LCL filter was studied, as it is a third-order system. The voltage control method reduces the voltage sag that occurs when an error appears or increases loads on the network. ANFIS gives overshoot (0.005%), settling time (0.02 sec), Peak time (0.02 sec), and improving THD from 3.21% to 2.33% compared with THD for the traditional PI controller, very excellent in filtering the power injected into the network from unwanted harmonics and reducing the THD to less than 5%, according to the international standard for IEEE 519-1992, in addition to that it is light in weight and low in cost compared to other types. Depending on the results obtained in this paper, the ANFIS results are much better than the PI controller, especially in non-linear applications. Since its voltage control remains almost constant, it does not change even after operating the load in the network.

Author contribution

All authors contributed equally to this work.

Funding

This research received no specific grant from any funding agency in the public, commercial, or not-for-profit sectors.

Data availability statement

The data that support the findings of this study are available on request from the corresponding author.

Conflicts of interest

The authors declare that there is no conflict of interest.

References

[1] Y. He, H. S.-H. Chung, C.-T. Lai, X. Zhang, and W. Wu, Active cancelation of equivalent grid impedance for improving stability and injected power quality of grid-connected inverter under variable grid condition, IEEE Trans. Power Electron, 33 (2018)9387-9398. https://doi.org/10.1109/TPEL.2018.2793459

[2] J. Xu, T. Tang, and S. Xie, Research on low-order current harmonics rejections for grid-connected LCL-filtered inverters, IET Power Electron. 7 (2014) 1227-1234. https://doi.org/10.1049/iet-pel.2013.0477

[3] W. Choi, W. Lee, D. Han, and B. Sarlioglu, New configuration of multifunctional grid-connected inverter to improve both current-based and voltage-based power quality, IEEE Trans. Ind. Appl., 54 (2018) 6374-6382. https://doi.org/10.1109/TIA.2018.2861737

[4] Y. Gui, Q. Xu, F. Blaabjerg, and H. Gong, Sliding mode control with grid voltage modulated DPC for voltage source inverters under distorted grid voltage, CPSS Trans. Power Electron. Appl., 4 (2019) 244-254, https://doi.org/10.24295/CPSSTPEA.2019.00023

[5] M. El-Habrouk, M. Darwish, and P. Mehta, Active power filters: A review, IEE Proceedings-Electric Power Applications, 147(2000) 403-413.

[6] H. Akagi, Active harmonic filters, Proceedings of the IEEE, 93 (2005) 2128-2141. https://doi.org/10.1109/JPROC.2005.859603

[7] H. Goh, M. Armstrong, and B. Zahawi, Adaptive control technique for suppression of resonance in grid-connected PV inverters, IET Power Electron. 12 (2019) 1479-1486. https://doi.org/10.1049/iet-pel.2018.5170

[8] M. N. Arafat, A. Elrayyah, and Y. Sozer, An effective smooth transition control strategy using droop-based synchronization for parallel inverters, IEEE Trans. Ind. Appl., 51 (2014) 2443-2454. https://doi.org/10.1109/TIA.2014.2369826

[9] A. B. Rad, W. L. Lo, and K. Tsang, Self-tuning PID controller using Newton-Raphson search method, IEEE Trans. Ind. Electron.,44 (1997)717-725. https://doi.org/10.1109/41.633479

[10] M. Tursini, F. Parasiliti, and D. Zhang, Real-time gain tuning of PI controllers for high-performance PMSM drives, IEEE Trans. Ind. Appl., 38 (2002)1018-1026, https://doi.org/10.1109/TIA.2002.800564

[11] V. A. Shankar, S. Umashankar, S. Padmanaban, S. Paramasivam, Adaptive neuro-fuzzy inference system (anfis) based direct torque control of pmsm driven centrifugal pump, Int. J. Renewable Energy Res. , 7 (2017) 1436-1447. https://doi.org/10.20508/ijrer.v7i3.5885.g7177

[12] W. A. A. Salem, G. F. Osman, and S. H. Arfa, Adaptive neuro-fuzzy inference system based field oriented control of PMSM & speed estimation, in Twentieth International Middle East Power Systems Conference (MEPCON), 2018, 626-631. https://doi.org/10.1109/MEPCON.2018.8635179

[13] A. Parviainen, J. Pyrhönen, and M. Niemelä, Axial flux interior permanent magnet synchronous motor with sinusoidally shaped magnets,Electromagnetic Fields in Electrical Engineering, (2002) 271.

[14] S. Hussain and M. A. Bazaz, Comparative analysis of speed control strategies for vector controlled PMSM drive, Int. Conf. Comput. Commun. Autom., Greater Noida, India, 2016, 1314-1319. https://doi.org/10.1109/CCAA.2016.7813950

[15] X. d. T. Garcia, B. Zigmund, A. A. Terlizzi, R. Pavlanin, and L. Salvatore, Comparison between FOC and DTC strategies for permanent magnet synchronous motors, Recent Adv. Electr. Electron. Eng. Recent., 5 (2011) 76-81.

[16] R. Krishnan, Electric motor drives: modeling, analysis, and control: Pearson, 2001.

[17] A. Darba, M. Esmalifalak, and E. S. Barazandeh, Implementing SVPWM technique to axial flux permanent magnet synchronous motor drive with internal model current controller, in 4th International Power Engineering and Optimization Conference (PEOCO), 2010, 126-131. https://doi.org/10.1109/PEOCO.2010.5559197

[18] K. Sitapati and R. Krishnan, Performance comparisons of radial and axial field, permanent-magnet, brushless machines, IEEE Trans. Ind. Appl., 37 (2001) 1219-1226. https://doi.org/10.1109/28.9524951`

[19] F. Daldaban and E. Çetin, Prototyping of axial flux permanent magnet motors,in 3rd Int. Symp. On Innovative Technologies in Engineering and Science (ISITES2015), Valencia, Spain, 2015.

[20] S. Nakashima, Y. Inagaki, and I. Miki, Sensorless initial rotor position estimation of surface permanent-magnet synchronous motor, IEEE Trans. Ind. Appl. 36 (2000) 1598-1603. https://doi.org/10.1109/28.887211

[21] F. Semiconductor, Sensorless PMSM vector control with a sliding mode observer for compressors using MC56F8013, Document Number, 2008.

[22] A. Verma, A. Singh, and A. Agrawal, Speed control of pmsm drive using anfis based speed controller, Development, 4 (2017).

[23] K. Jash, P. K. Saha, G. K. Panda, Vector control of permanent magnet synchronous motor based on sinusoidal pulse width modulated inverter with proportional integral controller, Int. J. Eng. Res. Appl., 3 (2013) 913-917.

[24] D. V. Lukichev, G. L. Demidova, A. Y. Kuzin, A. V. Saushev, Application of adaptive Neuro Fuzzy Inference System (ANFIS) controller in servodrive with multi-mass object, in 25th International Workshop on Electric Drives: Optimization in Control of Electric Drives (IWED), 2018,1-6. https://doi.org/10.1109/IWED.2018.8321388

[25] Joshi and A. P. Pius, ANFIS controller for vector control of three phase induction motor, Indones. J. Electr. Eng. Comput. Sci., 19 (2020) 1177-1185. https://doi.org/10.11591/ijeecs.v19.i3.pp1177-1185

[26] Zue, Aslain Ovono, and Ambrish Chandra. Simulation and stability analysis of a 100 kW grid connected LCL photovoltaic inverter for industry, 2006 IEEE Power Engineering Society General Meeting, Montreal, QC, Canada, 2006, pp. 6 pp.-. https://doi.org/10.1109/PES.2006.1709455

[27] IEEE Std 519-2014. Recommended Practice and Requirements for Harmonic Control in Electric Power Systems, in IEEE Std 519-2014 (Revision of IEEE Std 519-1992), 2014, 1-29.https://doi.org/10.1109/IEEESTD.2014.6826459